Estimating water turbidity from a smartphone camera

Lina Maria Lozano Wilches[1]
lina.lozano-wilches18@imperial.ac.uk
Chotiwat Jantarakasem[*2]
c.jantarakasem20@imperial.ac.uk
Lauré Sioné[2]
laure.sione09@imperial.ac.uk
Michael R. Templeton[2]
m.templeton@imperial.ac.uk
Krystian Mikolajczyk[1]
k.mikolajczyk@imperial.ac.uk

[1] Department of Electrical and Electronic Engineering ,
Imperial College London, UK

[2] Department of Civil and Environmental Engineering,
Imperial College London, UK

Abstract

Water quality monitoring is indispensable for safeguarding human health. One aspect of water quality is turbidity, the measurement of which typically involves on-site water sampling and laboratory analysis, which may be both costly and labour-intensive in the context of developing countries. Alternative portable devices have been developed but they are often inconvenient and require technical expertise. In recent years, smartphone-based solutions have been developed with the aim of bringing turbidimeters to the wider population. However, they rely on additional equipment to create enclosed environments for the sample and the camera to remove ambient light. Therefore, turbidimeters in general require either technical expertise or additional equipment, which has limited their usage, especially in developing countries, where they are most needed.

In this paper we introduce a new benchmark with a new task for computer vision that aims at estimating a blur of a pattern observed through a liquid. We propose and evaluate an approach for measuring water turbidity from a picture taken by a smartphone camera without any additional equipment. We design a simple protocol for taking a picture of a water sample that allows to estimate its turbidity, collect a dataset and design a benchmark for measuring the performance of computer vision methods in this task. Our model is able to accurately determine turbidity in the range of 0 - 40 NTU.

1 Introduction

Water is essential for the survival of humans, especially considering that the human body is about two-thirds water and it is used in most everyday activities [4] [12]. Not only is it important to have access to a water supply, but it is critical to ensure that it is also clean and

* Co-first author of this manuscript.

safe. For this, water quality monitoring is an indispensable step. One of the ways to measure this is by using turbidity, which is “a measure of the relative clarity of a liquid”[27].

Globally, one out of three people does not have access to safe drinking water [24]. While developed countries, like the UK, have strict regulations around the maximum turbidity levels [1], many developing nations fail to comply with the regulations and lack sufficient water sanitation infrastructures [7] [18]. However, the importance of water having low turbidity values is even more relevant, as poor sanitation and hygiene, contaminated water sources, and the overall poor quality of drinking water lead to disease and death amongst people of all ages [27].

Traditionally, turbidity measurements have involved on-site water sample collection and subsequent laboratory analysis, which is both labour-intensive and costly [22] [23]. There are alternative portable devices to test turbidity, but they require technical expertise due to the hazard of the standard preparation. In recent years, there has been a development of smartphone-based turbidimeters, but most of the solutions require additional equipment to create dark and closed environments to isolate the water sample from ambient light. Therefore, most of the alternatives require either technical expertise or additional equipment, which prevents ordinary users from monitoring turbidity.

In this paper we introduce a new task of water turbidity estimation with new data set, new benchmark and baseline results. We demonstrate that turbidity can be determined using only a smartphone camera. The user can take a picture of their water sample, and then, using a CNN network, predict the turbidity level. This solution is simple and can be widely accessed when considering that nearly 63% of the global population has access to a smartphone [28], with this number increasing annually. The contributions of this paper can be summarized as follows. We introduce a new task and a benchmark for estimating turbidity of a liquid. We propose a new approach for measuring the amount of blur in an image, based on an automatic preprocessing pipeline and a CNN model. We make available a new dataset with different characteristics and challenges. We provide an extensive evaluation and high accuracy results demonstrating that turbidity can be determined using only a smartphone-camera and a simple CNN architecture.

2 Related Work

In this section we first define the turbidity and discuss its usefulness is estimating the quality of water. We then review various methods for estimating turbidity.

2.1 Turbidity

Turbidity is a "measure of the relative clarity of a liquid" [27]. It detects the scattering or attenuation of light from a variety of sources. Turbidity is measured in Nephelometric Turbidity Units (NTU) [25]. The WHO has established that the turbidity of drinkable water should be no higher than 5 NTU and, ideally, lower than 1 NTU [25].

Turbidity has both water safety and aesthetic implications. It indicates the presence of suspended particulate matter (SPM) and other light-absorbing materials [6] that affect the transmission of a light beam in the water sample [9]. High turbidity represents a health concern, as it means that the water might contain particles that should not be consumed by humans, such as harmful pathogens like bacteria, which can affect human health and cause diseases[27]. It is important to note that high turbidity does not necessarily represent a direct threat to people's health [25], as well as low turbidity cannot be used as a complete guarantee of safe drinkable water. Nevertheless, turbidity is an extremely useful indicator that can provide valuable information about the quality of water quickly and on an ongoing basis in both small and large-scale drinking water treatment plants [25].

Other potential applications for estimating turbidity are around underwater computer vision [14], to remove turbidity for optical imaging [11], to acquire marine information using underwater imaging systems [8]. There are also attempts of improving early detection of neonatal sepsis by estimating turbidity in the blood serums of newborns [3]. In addition, there are applications for smart appliances where measuring turbidity allows to determine the amount of soil in clothes or dishes and "adapts the machine to save water, time, and energy, while providing superior cleaning performance" [10].

2.2 Related Papers

The related papers can be divided according to their relevance to the application, smartphone-based solutions for water quality monitoring, and to the blurring caused in the images by turbidity.

2.2.1 Application Related

While there are multiple smartphone-based methods for measuring the turbidity of water samples, common to most is the need for external equipment to isolate the water sample from ambient light. Even when some solutions could still be considerate cost-effective, the need for additional equipment limits access of these turbidimeters to the wider population.

Surface Tension. CapCam [30] is the only work that did not involve additional equipment other than a smartphone. The phone is placed on top of a paper cup with water. Using the smartphone's vibrations, capillary waves are generated. A picture with flash captures bright-and-dark patterns that can be seen at the bottom of the container, from which the surface tension of the water can be calculated. The inverse relationship between surface tension and water contamination allows to determine the contamination values [30]. Note that while turbidity and water contamination are not proportional to each other, an increase in turbidity can often indicate water contamination[25]. The model achieves high accuracy when pollution is caused by organic compounds, but it cannot sense inorganic contamination as it does not change surface tension. Also, the container needs to have a flat bottom, be light to vibrates, and circular. The model cannot work with non-transparent or coloured water.

Mie-scattering Principle. This is an optical approach based on the Mie-scattering principle where the light beam from an IR source hits a water sample. The scattered flux from this medium is monitored at a right angle to the direction of the incident beam by the smartphone IR detector. The irradiance of the scattered beam depends on the concentration of the μ-particles, which reflects turbidity. The smartphone and the water sample are held in a nylon plastic holder. It can measure turbidity in a wide range of 0 to 400 NTU and works for coloured mediums, except red, as this one affects the IR-detector response [15].

Mean Greyscale Index. A dark dark box was used in [26] and [13] to hold the water samples and capturing images, which are then converted into greyscale to calculate their mean greyscale index (MGI) assuming there is a linear relationship between MGI and turbidity. Similarly, [2] and [19] created smartphone attachments that contain optical fibers. These are used to transmit the collected scattered light to the camera sensor. From there, the light intensity of the spectrum is determined, and assuming the same linear MGI relationship, turbidity is estimated.

Colorimetric. Smartphone based estimation of water quality with a colorimetric method was proposed in [20]. Using a colour matching algorithm, the concentration level of each solution is calculated. The algorithm is limited by the training set, but it does not give accurate results in untrained samples [20].

2.2.2 Blurring and Deblurring

Water turbidity can be seen in images as blur [16]. Focusing on the blur as being uniform or Gaussian, [16] combines local and global features to estimate and reduce the blur. For non-uniform image blur, [6] segments the image into regions with homogeneous blur. Local blur estimators are applied using logistic regression and combined into a global estimate. Similarly, following a segmentation approach, the paper [29] uses a CNN and a GRNN to determine the image blur of each patch. The CNN determines the blur type, used by GRNN to determine the blur parameters. The approaches mentioned above were designed for land scenes. Another relevant area is underwater imaging, where deblurring of images poses its own challenge. A GAN with two encoder-decoder nets is used in [21] to improve image quality but it does not explicitly estimate the blur. Another form of enhancing by deblurring of images is by using a gradient guided filter in [17].

3 Method

In this section, we discuss the collection of data samples, the preprocessing pipeline and the proposed approach to estimating water turbidity.

3.1 Dataset Collection

Despite broad interest and diversity of applications that require estimating water turbidity there are no publicly available datasets for this task. To maximise the range of potential applications we collect the data using a smartphone camera, i.e., without any additional equipment. However a blur can only be observed on a non uniform background, we therefore design a simple pattern that allows to accurately estimate the blur.

We captured with a Samsung Galaxy Ultra S21 at a resolution for RGB of 3000x4000 in JPG. The camera was set to Pro Mode such that HDR, white balance, autofocus, flash, and magnification were deactivated to control focus and exposure conditions manually. All camera settings are kept fixed to minimize in-camera image processing that may affect the observed blur such as 1x zoom with fixed focus, no flash, ISO 50, shutter 1/15-1/30, exposure compensation, and white balance 3500K. The data, both train and test, is captured at high resolution to avoid introducing additional blur, to assure focus from a fixed distance and sufficient size of the cropped image sample that is used as an input to CNN. The samples were taken indoors. The water with different turbidity levels was created synthetically by combining various concentrations of formazine and kaolin clay with RO water. Colour could also be added on top of the formazine or kaolin clay solutions. We set the range between 0 and 40 NTU, which is the common range for drinkable water turbidimeters. Drinkable water should be below 5 NTU but ideally lower than 1 NTU, we use more levels within the safe drinking water range. Note that the difference in turbidity below 5 is not visible to a naked eye. The samples were collected for different containers including a 2.6cm tall glass vial that holds 20mL of water, a plastic darkly tinted Coca-Cola bottle or a clear plastic bottle, with 90mL of water. On the back of the container, a reference black on white pattern was placed to provide evidence of blur. This pattern was a circle of 3cm of diameter, referred to as the "dot", or "text", which was printed text of the common English pangram "A quick brown fox jumps over the lazy dog" in Helvetica of size 5. The dot can be easily drawn and a printed text can be extracted from newspapers, for example.

The water container was placed 10cm away from the camera to allow the full container and some white background to be seen in the images. One sets of images were taken using a tripod and voice recognition to trigger the capture. The images were annotated manually using the turbidity value from a compact turbidity meters instrument (CT12 model) [Palintest, UK].

Figure 1: Three dataset collection set-ups. Left: glass container, tripod and indoors. Middle: plastic bottle, tripod and indoors. Right: window, handheld smartphone and plastic bottle.

To create a more challenging dataset, the lighting and the handheld phone position were varied. The setting was moved next to the window to simulate the picture taken outside. Additionally, instead of using a tripod with a fixed position, the phone was handheld. Figure 1 shows the pattern and the data capturing setup.

3.2 Dataset Overview

Table 1 shows the main variations between each of the datasets and the total number of images after the preprocessing pipeline. The images used for training are 244x244 pixels for all datasets except the text dataset, which is 200x200 pixels. The total number of images are spread across eight different turbidity levels: 0, 1, 2.5, 4, 5, 7.5, 10 and 40 NTU. The number of images for each turbidity level are: turbidity(#images), 0(1816), 0.5(1305), 1(1616), 2(1822), 4(1806), 5(1812), 7.5(1812), 10(1828), 40(1584). We also added an additional class of 0.5 NTU in the formazine dataset to test the limits of the model. We refer to these two sets as 8 NTU and 9 NTU in the experiments. The results are reported of 8 NTU levels, without 0.5, unless specified otherwise. The noise of the labels is up to 10% and it is caused by limited accuracy in preparing the concentration of the stock solution, for example 20 NTU is in fact in range 18-22 NTU.

Dataset	Formazine	Kaolin Clay	Text	Plastic	Yellow	Natural	Natural Clear
1.Solution	F	KC	F	F	KC	F	F
2.Container	Glass	Glass	Glass	Plastic	Glass	Plastic	Clear Plastic
3.Background	Dot	Dot	Text	Dot	Dot	Dot	Dot
4.Colour	Clear	Clear	Clear	Clear	MO	Clear	Clear
5.Light	Lab	Lab	Lab	Lab	Lab	Window	Window
6.Tripod	Yes	Yes	Yes	Yes	Yes	No	No
#Images	15397	2149	2522	1256	5879	1224	1228

Table 1: Datasets collected. The solutions are represented by formazine (F) and kaolin clay (KC). Methyl orange (MO) produces a yellow water colour. For illumination, Lab represents the pictures taken under fluorescent light and window for pictures taken next to the window to represent natural light. Plastic indicates a tinted Coca-Cola plastic bottle unless specified otherwise e.g. clear plastic.

Water turbidity is measured by its transparency, and we estimate NTU by measuring the amount of blur in the background. A background with a step edge between black and white, such as in a black dot or printed text, allow to observe a blur in case the water is not perfectly transparent. A blur can be also produced by a convolution of a step edge with a Gaussian kernel, the size of which determines the resulting amount of blur on the edge. In fact, an experiment on a synthetic data with blur from a Gaussian kernel showed nearly perfect NTU prediction by our approach. Using a step edge makes it robust to the absolute values of black and white as well as the contrast and colour, thus illumination conditions. For the data with the dot background, the images are centred on the dot, which is aligned with the centre of the container as this is the area with the least distortions from the container. From each original image, two image crops are extracted: one centred on the upper edge of the dot, and another, symmetric with the lower edge of the dot. For the text background, two final crops per each original image were extracted i.e., containing text: *The quick brown fox* and the second one with *jumps over the lazy dog*.

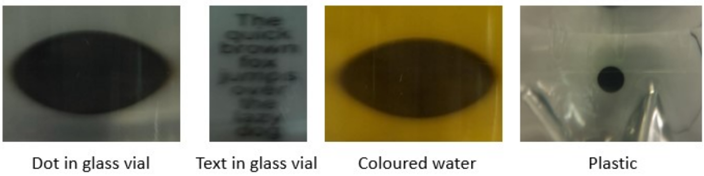

Figure 2: Cropped pictures from the different datasets. The F and KC datasets are reflected by the dot in glass vial. The plastic picture represents the plastic, natural or natural clear datasets.

Formazine dataset represents the most controlled conditions and least noise from external factors such as container and illumination.
Kaolin Clay dataset was created using a solution of inorganic suspended solids. KC particles reflect light, therefore the blur in the images is more difficult to measure in images.
Text dataset explores the performance of the model by using a different background that inludes many small edges.
Plastic dataset increases the complexity due to a plastic Coca-Cola bottle of 500mL. It has a non-covex shape, it is tinted and requires a larger amount of water. However, this container is widely available in most geographic locations.

Yellow dataset was obtained from different turbidity concentrations mixed with methyl orange in 1, 2.5 and 5 PPM to generate various intensities of coloured water.
Natural dateset represents more "natural" lighting conditions with images taken by a window. A tinted Coca-Cola water bottle was used.
Natural Clear dataset is also in natural light, except the plastic Coca-Cola bottle was clear.

WaTur: Our collected **Wa**ter **Tur**bidity dataset is available online[1].

3.3 Preprocessing

The aim of the preprocessing pipeline was to remove the unnecessary elements of the original image and create smaller images that focus only on the parts where the blur is best seen i.e., dot or text. To create a pipeline robust to the movements of the water container and background, the process had to be able to detect the dot from the original image and then crop around it. a) The bottom of the image is cropped to remove the "feet" of the container. b) brightness is enhanced to increased the contrast between the black dot and the rest of the image. c) morphological operations: opening (erosion + dilatation) and closing (inverse of opening, dilatation + erosion) are performed to find the actual shape and size of the background. d) As the black contours are detected, the next step is to filter according to area and perimeter for the dot background. For the text background, no filtering is done and the contours are simply merged due to the differences in the letter's shape. e) The filtered contours are enclosed in a rectangle that fits tightly to the required shape. 100 pixels are added to each of the sides to guarantee that the edges of the contours are included in the picture. f) The images are normalised by using as the mean the centre of the black dot area, and the cropped rectangle as the variance of the image. g) the cropped rectangular RGB image is cropped again into two smaller centred squares.

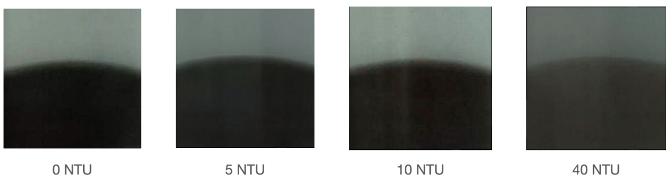

Figure 3: Sample pictures after preprocessing for different NTU for F dataset.

3.4 Model Architecture

We propose a small model to make the inference as efficient as possible. The architecture consists of five convolutional layers with increasing depth (16 - 256) and each filter size is 3x3. ReLU was used as the activation function in all layers, and average pooling was used in between each convolutional layer. We experimented with two different heads: a classification head of the size of the number of classes and softmax on the output, and a regression head of size one and linear output. The batch size was fixed to 32, and the training and validation split was 80/20% within each dataset. Adam, with learning rate and decay rate of 0.001, was used as the optimizer. The classification pipeline was trained on categorical cross-entropy and the regression model was trained using mean squared error. We compare the two models

[1] https://github.com/lml418/WaTur-Water-Turbidity-Dataset

using the accuracy i.e., the number of correctly classified samples to the total number of samples. For the regression model the accuracy was calculated by quantizing the real valued prediction into the closest discrete class i.e., the same as in the classification, and comparing to the ground truth. Root mean square error (RMSE) between the prediction and the ground truth (gt) $\sqrt{\frac{1}{N}\sum(predicted-gt)^2}$ was calculated for both problems as an additional metric. For the classification model, the predicted label with the highest probability was selected.

4 Results

In this section an analysis on the performance of the simple CNN architecture under different dataset will be carried.

Formazine Dataset. This first dataset had the most controlled conditions and the model achieved high accuracy even when dealing with turbidities as small as 0.5 NTU, impossible to differentiate naked eye, showing that the model is able to determine turbidity. Performance drops by nearly 30% when addressing this problem as a regression task as shown in table 2.

Models	#Images	Acc (%)	RMSE
8 NTU Classification	14092	97.48	0.0520
8 NTU Regression	14092	69.93	0.6004
9 NTU Classification	15397	97.34	0.0559
9 NTU Regression	15397	64.55	0.7470

Table 2: Results for formazine classification and regression after 10 epochs. High accuracy and performance for both of the classification problems. Performance drops for the regression based approach.

Text Dataset. By changing the background to text, the model is still able to achieve a high performance. Nevertheless, the accuracy is slightly lower when tested for the same number of epochs and trained using the same number of per class examples. The blur seems to be easier to see in the dot that in text as even when comparing both background under RO water (equivalent to 0 NTU), the text is already blurry. Additionally, from an application perspective it is easier to draw a dot, therefore the dot was chosen as the ideal background.

Models	Dot Classification	Text Classification
#Images	2522	2522
Acc (%)	96.43	93.65
RMSE	0.2046	0.4087

Table 3: Comparison for dot and text formazine classification at 40 epochs. Classification when using the dot as background achieves slightly better performance than for text.

Kaolin Clay Dataset. Formazine (F) is representative of organic suspended solids. As the model achieved high performance for this solution, the next step was to test the model for inorganic suspended solids ie., Kaolin Clay (KC).

Test 1 showed that the model trained on F cannot be directly used for inference KC. This is to be expected when considering that KC contains larger particles which reflect light so the pictures show the difference in turbidity with lower effects. Indeed, the model was predicting 1 NTU for all KC images. Test 2 shows the results of the model trained with KC that achieves a good performance but slightly lower than with the formazine dataset in Table 2 as the task is more challenging.

	Test 1	Test 2
Train data	Formazine	Kaolin Clay
#Images	14092	2149
Acc (%)	2.93	91.16
RMSE	42.9195	0.3300

Table 4: Classification results for training on kaolin and formazine [3]. Kaolin clay samples reflect light so the model trained on formazine cannot be used. However, in test 2, the model trained on KC can extract and learn the characteristics from kaolin clay leading to high accuracy.

Plastic Dataset. A plastic bottle is a more ubiquitous container than a clear glass vial. This dataset provided the following conclusions: 1) Test 1. The model trained using data samples of the glass vial cannot be directly applied to plastic even if the other conditions are the same. 2) Test 2. The model is able to solve the dataset with high accuracy, the highest out of all the previously tested datasets. this can be due to the fact that the glass vial has higher curvature which introduces more noise blur noise than the larger plastic bottle. 3) Test 3. The model performs better for the same test images when using F and KC together as the training set. 4) Test 4. The model achieves high accuracy when trained on a mixture of datasets.

Test	Test 1	Test 2	Test 3	Test 4
Pictures used for training	F	F	F & KC	F & KC
Container	Glass	Plastic	Glass	Plastic & Glass
#Images	14092	1256	16040	18189
Acc (%)	11.16	99.20	20.72	96.15
RMSE	22.7563	0.2047	27.7628	0.6747

Table 5: Classification results for different solutions and containers.

Yellow Dataset. This experiment tests the model's ability to generalise to different coloured water. Note that, coloured water does not necessarily have higher turbidity than clear water. From training only on clear water samples and testing on coloured water without any data augmentations, it can be concluded that the model is unable to generalise to a different colour. However, when trained on a mixture of clear and coloured water, the model achieves again high performance.

Training Images	Kaolin Clay	Kaolin Clay + Methyl Orange
#Images	2149	5897
Acc (%)	15.60	98.05
RMSE	1046.1393	0.0964

Table 6: Results for dot kaolin clay glass vial with methyl orange. The weights of kaolin clay for clear water cannot be directly applied to water with colouring. However, when training in a mix of water samples, the model achieves high accuracy for clear and coloured water samples.

[3]Note that the total number of images for Formazine + Kaolin has exactly 201 samples less than the sum of the samples for each compound. This is due to the fact that the samples for 0 NTU are the same for both as they use RO water.

Natural Dataset. This dataset was created to see the impact of changing the conditions to natural light and handheld smartphone instead of using a tripod as well as different plastic bottle. The remaining conditions were the same as in the plastic dataset. As seen in table 7, the model achieves high accuracy when trained under those conditions. Performance drops compared to the plastic dataset which can be explained by the more noise caused by the handheld camera motion and the lighting conditions which cause more reflections and illumination patches as the light coming from the window affected more one side of the bottle than the other.

Dataset	Natural tinted	Natural clear
#Images	1224	1228
Acc (%)	95.92	99.59
RMSE	0.3188	0.0180

Table 7: Results for dot formazine plastic bottle under natural lighting conditions classification.

5 Conclusion and Future Work

This study successfully demonstrates that water turbidity can be estimated with high accuracy by only using a smartphone-camera and a simple CNN architecture. Different datasets under various lab controlled conditions were taken to evaluate the performance of the model. A simple CNN architecture achieves high performance when trained from a sample of that dataset for turbidity in the range between 0 to 40 NTU. We do not expect significant divergence in terms of performance if the sample capturing conditions are similar. The experiments were conducted in a way to reproduce field conditions as closely as possible. These include two main types of water turbidity that are considered in civil engineering (formazine and clay), different colours, indoor settings, natural and artificial illumination, glass and plastic containers of different shapes, a smartphone and a simple background.

Future work include further relaxation of the controlled conditions to make the methodology for the data collection simpler for its exploitation in the field. Additionally, there are possible extensions such as data augmentation or domain adaptation to improve the generalisation properties. This project continues with collection of tap water samples in developing countries where turbidity often exceeds 4 NTU. Other applications such as underwater imagery can also benefit from accurate estimation of water turbidity.

Acknowledgement. This research was jointly supported by Chist-Era, UK EPSRC project EP/S032398/1 and the Scholarship in Commemoration of Her Royal Highness Princess Chulabhorn's 60th Birthday Anniversary under HRH Princess Chulabhorn College of Medical Science, Chulabhorn Royal Academy.

References

[1] The water supply (water quality) regulations 2016, 2016. (SI 2016/614).

[2] Abdullah Bayram, Eyyup Yalcin, Serafettin Demic, Orhan Gunduz, and Mehmet Ertugrul Solmaz. Development and application of a low-cost smartphone-based turbidimeter using scattered light. *Appl. Opt.*, 57(21):5935–5940, Jul 2018. doi: 10.1364/AO.

57.005935. URL http://www.osapublishing.org/ao/abstract.cfm?URI=ao-57-21-5935.

[3] Daniel Benalcazar, Luis Eguiguren, María B. Alvarez, Estela Arteaga, Fernando Jácome, and Michelle Grunauer. Design of an electronic device for turbidity detection in blood serum in newborns. In *2016 IEEE Ecuador Technical Chapters Meeting (ETCM)*, pages 1–4, 2016. doi: 10.1109/ETCM.2016.7750852.

[4] Claude E. Boyd. *Water Quality An Introduction*. Springer International Publishing, Cham, 3 edition, 2020. ISBN 9783030233358. doi: 10.1007/978-3-030-23335-8. ID: alma991000320992801591.

[5] Health Canada. Guidelines for canadian drinking water quality: Guideline technical document - turbdity, 2012. URL https://www.canada.ca/content/dam/hc-sc/migration/hc-sc/ewh-semt/alt_formats/pdf/pubs/water-eau/sum_guide-res_recom/sum_guide-res_recom-eng.pdf.

[6] Florent Couzinié-Devy, Jian Sun, Karteek Alahari, and Jean Ponce. Learning to estimate and remove non-uniform image blur. In *2013 IEEE Conference on Computer Vision and Pattern Recognition*, pages 1075–1082, 2013. doi: 10.1109/CVPR.2013.143.

[7] Jonny Crocker and Jamie Bartram. Comparison and cost analysis of drinking water quality monitoring requirements versus practice in seven developing countries. *International Journal of Environmental Research and Public Health*, 11(7):7333–7346, 2014. ISSN 1660-4601. doi: 10.3390/ijerph110707333. URL https://www.mdpi.com/1660-4601/11/7/7333.

[8] Zhi Deng, Daxiong Ji, Lizhong Gu, Mingzhe Sun, and Xin Yao. Underwater image enhancement algorithm adapted to different turbidities ranges. In *2018 IEEE 8th International Conference on Underwater System Technology: Theory and Applications (USYS)*, pages 1–6, 2018. doi: 10.1109/USYS.2018.8778882.

[9] John Downing. *Turbidity Monitoring*, chapter 24, pages 511–546. John Wiley & Sons, Ltd, 2004. ISBN 9780471473336. doi: https://doi.org/10.1002/0471473332.ch24. URL https://onlinelibrary.wiley.com/doi/abs/10.1002/0471473332.ch24.

[10] T. Erickson. Turbidity sensing as a building block for smart appliances. *IEEE Industry Applications Magazine*, 3(3):31–36, 1997. doi: 10.1109/2943.589891.

[11] Vijay Kumar Gowda, Vivek Maik, K. Karibassappa, and Joonki Paik. Removal of underwater turbidity using an optical imaging platform. In *2016 International Conference on Electronics, Information, and Communications (ICEIC)*, pages 1–5, 2016. doi: 10.1109/ELINFOCOM.2016.7562931.

[12] Ralph P. Hall, Barbara Van Koppen, and Emily Van Houweling. The human right to water: The importance of domestic and productive water rights. *Science and Engineering Ethics; Sci Eng Ethics*, 20(4):849–868, 2013. doi: 10.1007/s11948-013-9499-3. ID: cdi_proquest_journals_1626120424.

[13] Farah Najihah Hamidi, Mohamad Faiz Zainuddin, Zulkifly Abbas, and Ahmad Fahad Ahmad. Low cost and simple procedure to determine water turbidity with image processing. In *Proceedings of the International Conference on Imaging, Signal Processing and Communication*, ICISPC 2017, page 30–34, New York, NY, USA, 2017. Association for Computing Machinery. ISBN 9781450352895. doi: 10.1145/3132300.3132302. URL https://doi.org/10.1145/3132300.3132302.

[14] Jonathan Horgan and Daniel J. F. Toal. Computer vision applications in the navigation of unmanned underwater vehicles. 01 2009. ISBN 978-953-7619-49-7. doi: 10.5772/6703.

[15] Iftak Hussain, K. U. Ahamad, and P. Nath. Water turbidity sensing using a smartphone. *Royal Society of Schemistry Advances*, 6:22374–22382, 2016. URL https://www.academia.edu/33455542/Water_turbidity_sensing_using_a_smartphone?pop_sutd=false.

[16] A. Chrispin Jiji and M Vivek. Underwater turbidity removal through ill-posed optimization with sparse modeling. In *2017 IEEE International Conference on Power, Control, Signals and Instrumentation Engineering (ICPCSI)*, pages 1865–1869, 2017. doi: 10.1109/ICPCSI.2017.8392039.

[17] A.Chrispin Jiji and R Nagaraj. Enhancement of underwater deblurred images using gradient guided filter. In *2018 3rd IEEE International Conference on Recent Trends in Electronics, Information & Communication Technology (RTEICT)*, pages 1136–1140, 2018. doi: 10.1109/RTEICT42901.2018.9012305.

[18] Sabrina Kirschke, Tamara Avellán, Ilona Bärlund, Janos J. Bogardi, Laurence Carvalho, Deborah Chapman, Chris W. S. Dickens, Kenneth Irvine, SungBong Lee, Thomas Mehner, and Stuart Warner. Capacity challenges in water quality monitoring: understanding the role of human development. *Environmental Monitoring and Assessment*, 192(5):298, April 2020. ISSN 1573-2959. doi: 10.1007/s10661-020-8224-3. URL https://doi.org/10.1007/s10661-020-8224-3.

[19] Hatice Ceylan Koydemir, Simran Rajpal, Esin Gumustekin, Doruk Karinca, Kyle Liang, Zoltan Göröcs, Derek Tseng, and Aydogan Ozcan. Smartphone-based turbidity reader. *Scientific Reports*, 9(1):19901, 2019. doi: 10.1038/s41598-019-56474-z. URL https://doi.org/10.1038/s41598-019-56474-z. ID: Ceylan Koydemir2019.

[20] Volkan Kılıç, Gazihan Alankus, Nesrin Horzum, Ali Y. Mutlu, Abdullah Bayram, and Mehmet E. Solmaz. Single-image-referenced colorimetric water quality detection using a smartphone. *ACS Omega*, 3(5):5531–5536, 2018. doi: 10.1021/acsomega.8b00625. URL https://doi.org/10.1021/acsomega.8b00625. PMID: 31458756.

[21] Tengyue Li, Shenghui Rong, Bo He, and Long Chen. Underwater image deblurring framework using a generative adversarial network. In *OCEANS 2022 - Chennai*, pages 1–4, 2022. doi: 10.1109/OCEANSChennai45887.2022.9775336.

[22] O. Korostynska A. Mason and A. I. Al-shamma. *Smart sensors for real-time water quality monitoring*, volume 4. Springer, 2013 edition, 2013. ISBN 9783642370052.

[23] Darragh Mullins, Derek Coburn, Louise Hannon, Edward Jones, Eoghan Clifford, and Martin Glavin. A novel image processing-based system for turbidity measurement in domestic and industrial wastewater. *Water Science and Technology*, 77(5):1469–1482, 01 2018. ISSN 0273-1223. doi: 10.2166/wst.2018.030. URL https://doi.org/10.2166/wst.2018.030.

[24] United Nations. Un sustainable development goals - goal 6: Clean water and sanitation, 2018. URL https://www.un.org/sustainabledevelopment/water-and-sanitation/.

[25] World Health Organization. Water quality and health - review of turbidity: Information for regulators and water suppliers, Feb 20, 2017. URL https://www.who.int/water_sanitation_health/publications/turbidity-information-200217.pdf.

[26] Siti Nor Asyiqin Ramli, Khairunnisa Kadaruddin, Mohamad Faiz Zainuddin, and Zulkifly Abbas. The development of low cost turbidimeter using smartphone camera and image processing. *International Jounal of Innovative Technology and Exploring Engineering (EJITEE)*, 8(9S):420–424, June 2019. URL https://www.ijitee.org/wp-content/uploads/papers/v8i8s/H10720688S19.pdf.

[27] Water Science School. Turbidity and water, 6 June, 2018. URL https://www.usgs.gov/special-topics/water-science-school/science/turbidity-and-water.

[28] Laura Silver. Smartphone ownership is growing rapidly around the world, but not always equally, Feb 5, 2019. URL https://www.pewresearch.org/global/2019/02/05/smartphone-ownership-is-growing-rapidly-around-the-world-but

[29] Ruomei Yan and Ling Shao. Blind image blur estimation via deep learning. *IEEE Transactions on Image Processing*, 25(4):1910–1921, 2016. doi: 10.1109/TIP.2016.2535273.

[30] Shichao Yue and Dina Katabi. Liquid testing with your smartphone. In *Proceedings of the 17th Annual International Conference on Mobile Systems, Applications, and Services*, MobiSys '19, page 275–286, New York, NY, USA, 2019. Association for Computing Machinery. ISBN 9781450366618. doi: 10.1145/3307334.3326078. URL https://doi.org/10.1145/3307334.3326078.